SUPPLEMENTAL INFORMATION

SUPPLEMENTAL FIGURES

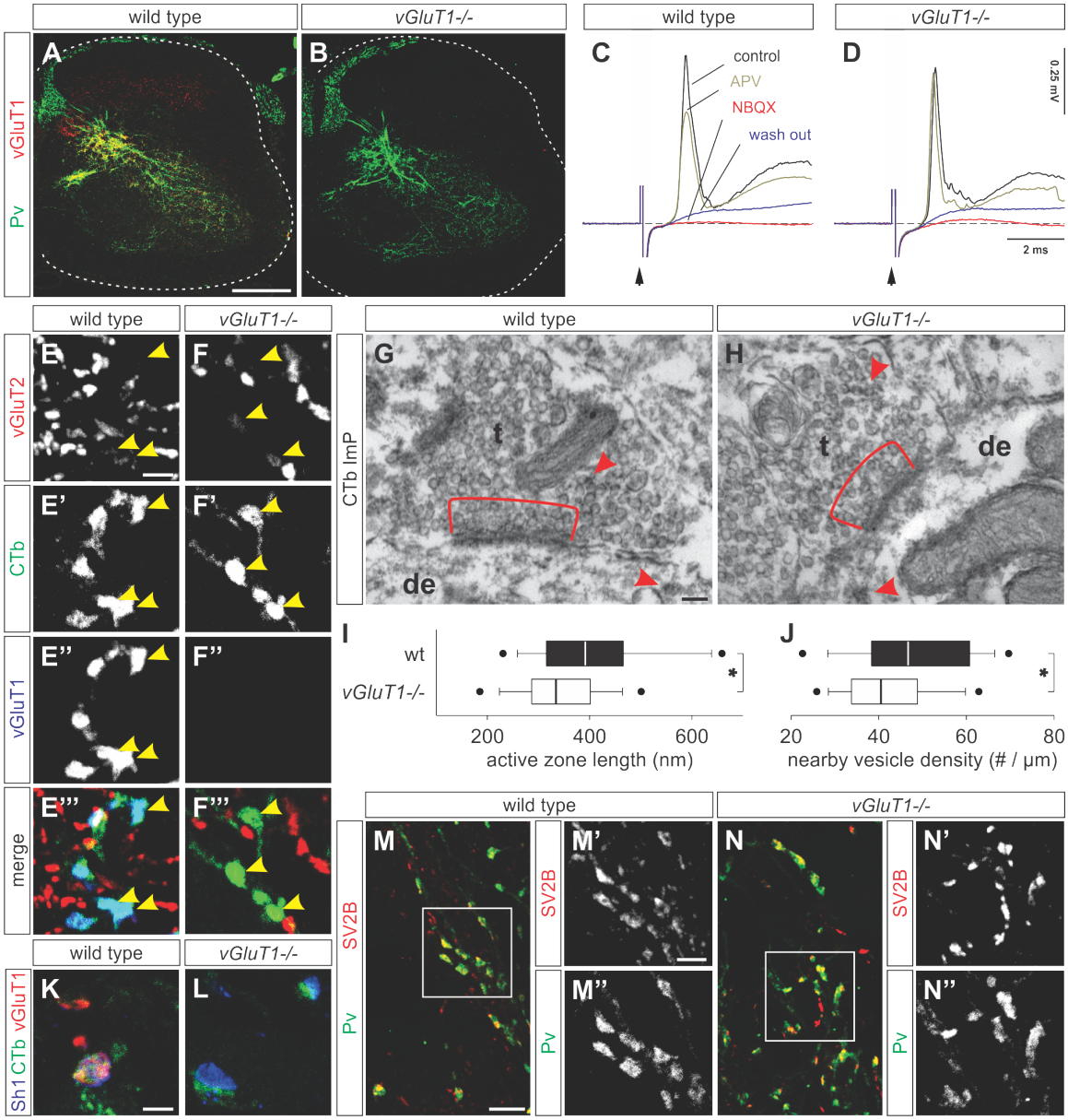

Figure S1. Related to Figure 1: Sensory neurons form synapses in *vGluT1-/-* mice.
(A and B) Pv^{ON} (green) sensory afferent projections in p12 wt (A) and *vGluT1-/-* (B) spinal cords at L4-L5. Note absence of vGluT1 (red in wt) in *vGluT1-/-* mice.
(C and D) Pharmacological exposure to the glutamate receptor antagonists NBQX (blocks AMPA receptors) and APV (blocks NMDA receptors) revealed that the monosynaptic reflex remains glutamatergically-mediated in *vGluT1-/-* (D) as compared to wt (C) mice. Superimposed ventral root responses following dorsal root stimulation under APV (100 µM, in green) and NBQX (20 µM, in red). Black arrows indicate the stimulus artifact.
(E-F''') vGlut2 (red) is expressed in CTb^{ON} (green) proprioceptive sensory terminals in p12 ventral spinal cords of wt (E-E''') and *vGluT1-/-* (F-F''') mice (yellow arrowheads).
(G and H) CTb immunoperoxidase labeling (CTb ImP; red arrowheads) in both proprioceptive afferent terminals and motor neuron dendrites in wt (G) and *vGluT1-/-* (H) mice.

(I and J) Measurement of AZ length (I) and density (J) of synaptic vesicles near the AZ in proprioceptive sensory terminals of p12 wt and *vGluT1-/-* mice. AZ length and vesicle density near AZ are slightly reduced in *vGluT1-/-* mice (I: AZ: *n*(wt) = 40 boutons, 3 mice; *n*(*vGluT1-/-*) = 43 boutons, 3 mice; Mann-Whitney Rank Sum, $p = 0.03$ *; J: vesicle density: *n*(wt) = 40 boutons, 3 mice; (vesicle density): *n*(*vGluT1-/-*) = 43 boutons, 3 mice; Mann-Whitney Rank Sum, $p = 0.041$ *). All vesicles within 125 nm, or the width of 3 vesicles, were counted (red brackets in G and H). Vesicle counts were normalized to the length of the postsynaptic density. t, sensory afferent terminal; de, motor neuron dendrite.
(K and L) CTb^{ON} (green) sensory afferent terminals are juxtaposed to postsynaptic Shank1a (Sh1, blue) in p21 wt (K) and *vGluT1-/-* (L) spinal cords. In contrast to wt mice, *vGluT1-/-* spinal cords are completely devoid of vGluT1 (red).
(M-N'') Sensory terminals in p12 wt (M-M'') and *vGluT1-/-* (N-N'') spinal cords are positive for SV2B (red; rabbit anti-SV2B 1:3000 (Synaptic Systems Cat# 119 102 RRID, AB_2196884)) and Pv (green).
Scale bars: 250 µm (A, B), 2.5 µm (E-F''', K, L), 100 nm (G, H), 5 µm (M-N''). Lines and whiskers on box diagrams represent data between 9th and 91st percentile, dots show the 5th and 95th percentile.

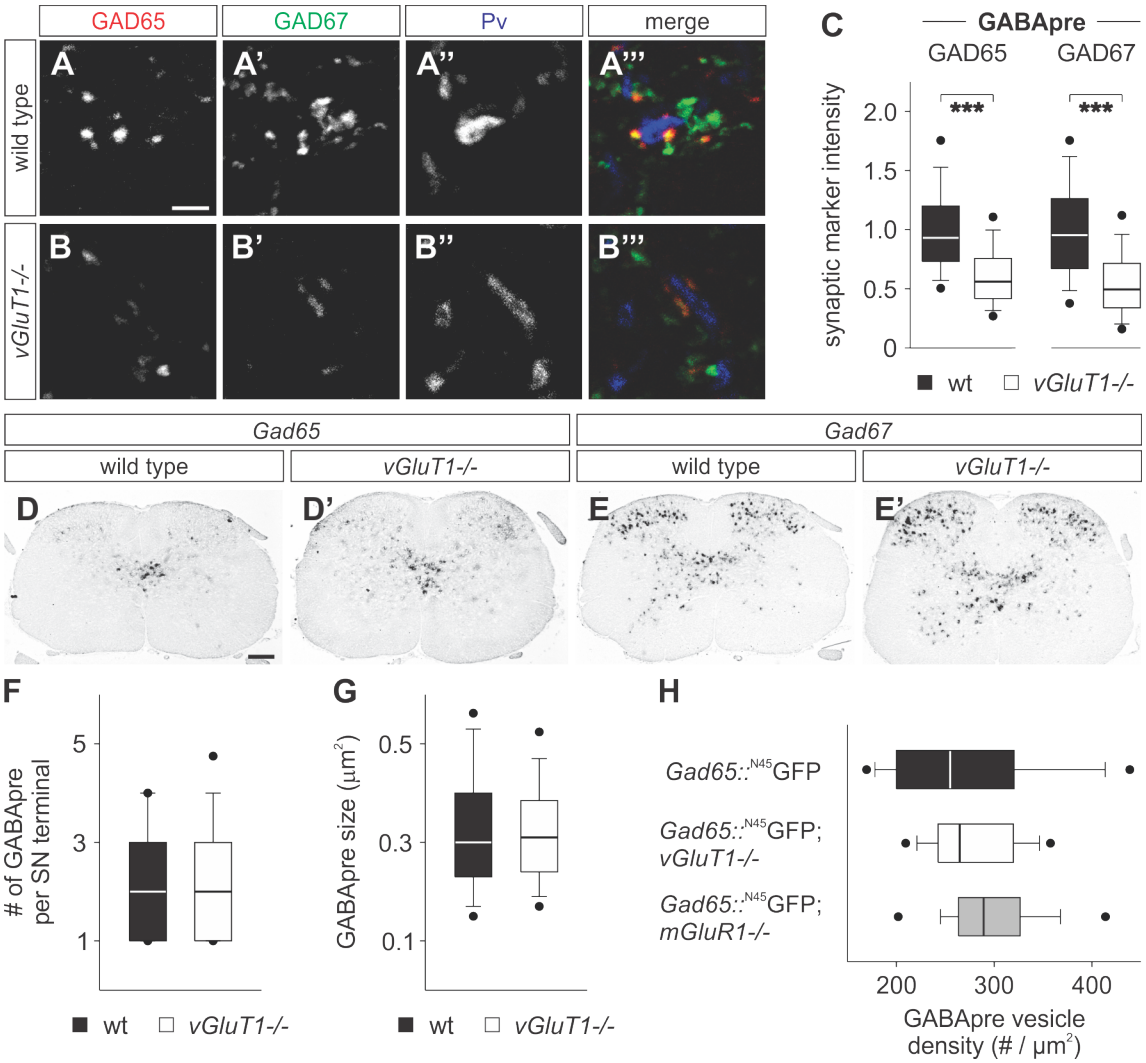

Figure S2. Related to Figure 2: Characterization of GABApre terminals in *vGluT1-/-* mice.
(A-B''') Immunoreactivity of GAD65 (red) and GAD67 (green) in GABApre terminals contacting Pv (blue) proprioceptive afferent terminals of p12 wt (A-A''') and *vGluT1-/-* (B-B''') mice.
(C) Synaptic marker intensity measurements in GABApre terminals at p12. GAD65 and GAD67 levels in GABApre terminals are reduced in *vGluT1-/-* as compared to wt mice. Data shown normalized with respect to wt data (GAD65: n(wt) = 592 boutons, 3 mice; n(*vGluT1-/-*) = 540 boutons, 6 mice; Mann-Whitney Rank Sum, $p < 0.001$ ***; GAD67: n(wt) = 446 boutons, 3 mice; n(*vGluT1-/-*) = 473 boutons, 6 mice; Mann-Whitney Rank Sum, $p < 0.001$ ***). GAD67 levels in GABApost terminals are unchanged (data not shown).
(D-E') *Gad65* and *Gad67 in situ* on p21 wt and *vGluT1-/-* spinal cords.
(F and G) Quantification of the number and size of GABApre terminals in p12 wt and *vGluT1-/-* L5 spinal segments. The number (F; n(wt) = 159 boutons, 3 mice; n(*vGluT1-/-*) = 144 boutons, 3 mice; Mann-Whitney Rank Sum, $p = 0.85$ NS) and size (G; n(wt) = 147 boutons, 3 mice; n(*vGluT1-/-*) = 205 boutons, 3 mice; Mann-Whitney Rank Sum, $p = 0.83$ NS) of GABApre terminals is the same in *vGluT1-/-* and wt mice.
(H) Synaptic vesicle density in GABApre terminals in *Gad65::*^{N45}GFP; *vGluT1-/-* and *Gad65::*^{N45}GFP; *mGluR1-/-* mice is unchanged, as compared to *Gad65::*^{N45}GFP control mice (n(*Gad65::*^{N45}GFP) = 23 boutons, 3 mice; n(*Gad65::*^{N45}GFP; *vGluT1-/-*) = 23 boutons, 3 mice; n(*Gad65::*^{N45}GFP; *mGluR1-/-*) = 24 boutons, 3 mice; One-way ANOVA, $p = 0.18$ NS).
Scale bars: 2.5 µm (A-B'''), 100 µm (D-E'). Error bars represent s.e.m. Lines and whiskers on box diagrams represent data between 9th and 91st percentile, dots show the 5th and 95th percentile.

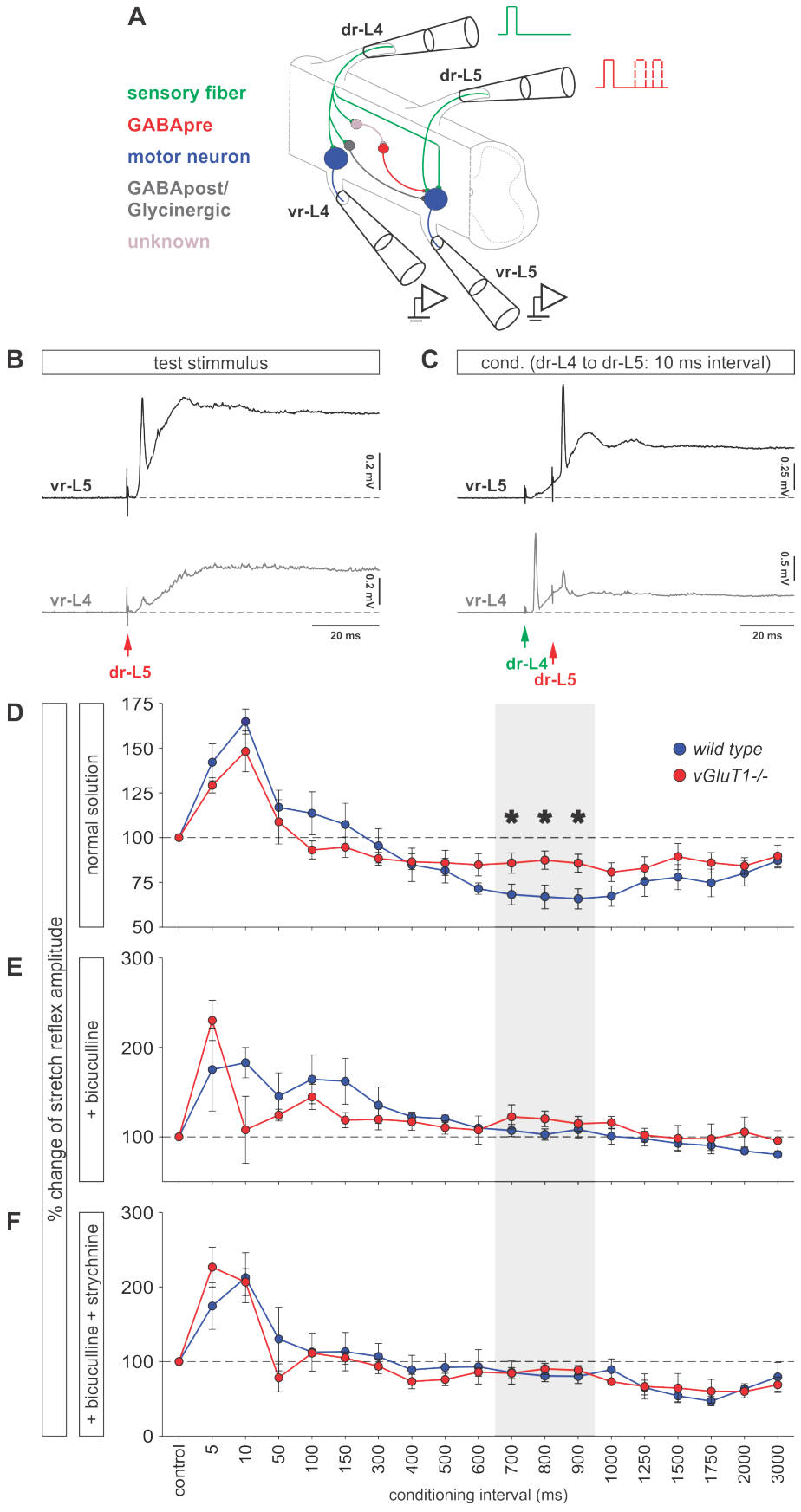
A
sensory fiber
GABApre
motor neuron
GABApost/
Glycinergic
unknown
dr-L4
dr-L5
vr-L4
vr-L5
B
test stimmulus
vr-L5
0.2 mV
vr-L4
0.2 mV
20 ms
dr-L5
C
cond. (dr-L4 to dr-L5: 10 ms interval)
vr-L5
0.25 mV
vr-L4
0.5 mV
20 ms
dr-L4
dr-L5
D
normal solution
wild type
vGluT1-/-
E
+ bicuculline
F
+ bicuculline + strychnine
% change of stretch reflex amplitude
conditioning interval (ms)
control
5
10
50
100
150
300
400
500
600
700
800
900
1000
1250
1500
1750
2000
3000

Figure S3. Related to Figure 3: Conditioning protocol to assess presynaptic inhibition.
(A) Schematic of the experimental protocol to test presynaptic inhibition. Dorsal roots L4 and L5 as well as their homosegmental ventral roots were placed in tight fitting suction electrodes. Sensory fibers (dr-L4, dr-L5) were stimulated at maximal intensity to record the maximum monosynaptically-mediated response from motor neurons (vr-L4, vr-L5). For simplicity, the key neurons activated in this pathway are color-coded.
(B) Averaged responses (5 at 0.1 Hz) from the L5 (black trace) and L4 (grey trace) ventral root following stimulation of the dr-L5 (stimulus artifact is denoted by red arrow). Activation of the dr-L5 monosynaptically-activated motor neurons in the same segment (monitored by vr-L5 response) and to a smaller extent motor neurons in the adjacent segment (monitored by vr-L4).
(C) The dr-L5 to vr-L5 reflex was conditioned by stimulation of the dr-L4 (see green arrow) prior to the dr-L5 stimulation. The conditioning interval was 10 ms. Monitoring of the vr-L4 response ensured that proprioceptive fibers in the dr-L4 were maximally stimulated due to the presence of the monosynaptic reflex in vr-L4.
(D-F) Percentage change of the monosynaptic reflex amplitude for the different conditioning intervals tested (range: 5 ms to 3 s) in normal solution (D), under 10 µM bicuculline (E) and under 10 µM bicuculline and 10 µM strychnine (F) in wt (blue, $n = 5$, p12) and *vGluT1-/-* (red, $n = 4$, p12) mice.

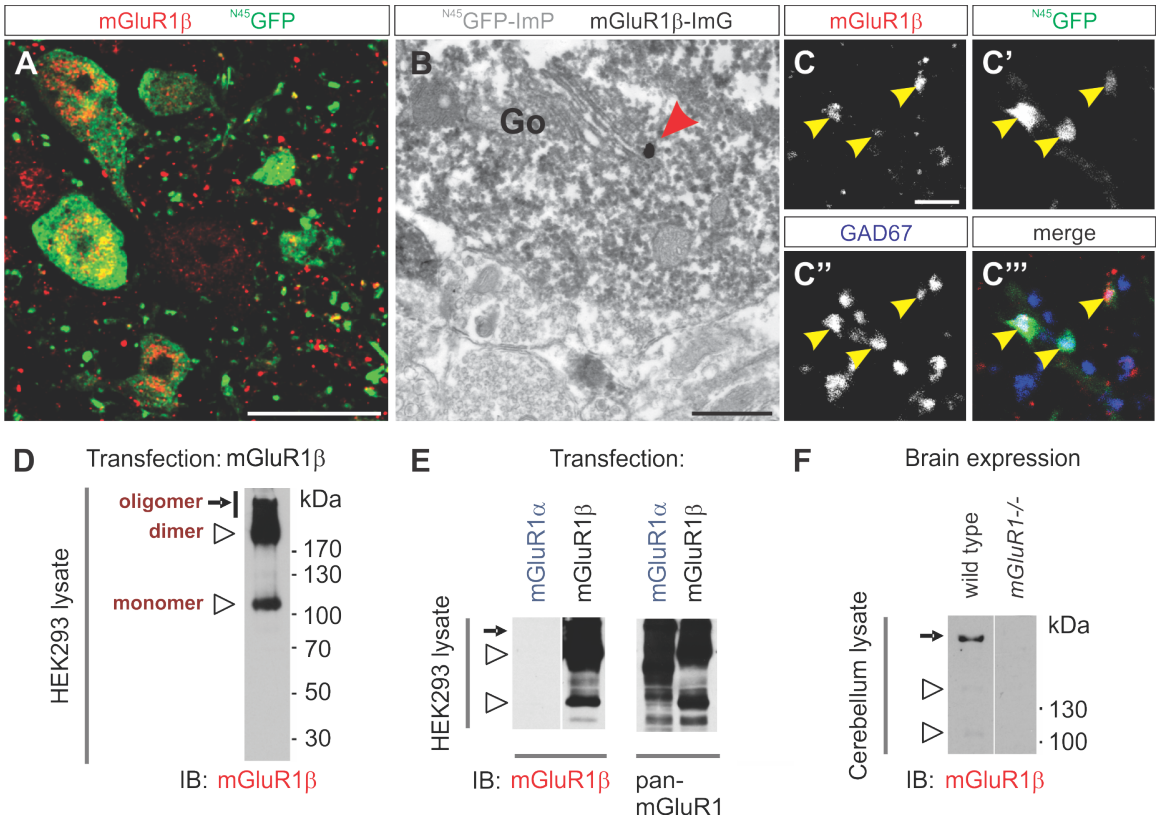

Figure S4. Related to Figure 4: mGluR1β expression in GABApre neurons and terminals.

(A) mGluR1β (red) is expressed in a subset of $^{N45}GFP^{ON}$ interneurons (green) in the intermediate spinal cord of p21 *Gad65::*^{N45}GFP mice.

(B) mGluR1β immunogold particle (mGluR1β-ImG; red arrowhead) in ^{N45}GFP immunoperoxidase (^{N45}GFP-ImP) cell body. Particles were often observed in association with endomembranes, such as a portion of the Golgi apparatus (Go) shown here. Image from L4-L5 spinal cords of p21 mice.

(C-C''') mGluR1β (red) overlaps with GABApre terminal marker GAD67 (blue) in $^{N45}GFP^{ON}$ (green) GABApre terminals (yellow arrowheads indicate mGluR1β, GFP and GAD67 co-labeling).

(D-F) Characterization of anti-mGluR1β antibody. (D) Anti-mGluR1β recognizes recombinant rat mGluR1β (Tanabe et al., 1992) under denaturing conditions. Representative immunoblot in which open arrowheads indicate mGluR1β monomers (≈ 100 kDa) and dimers (≈ 200 kDa) and arrow indicates higher molecular mass oligomers. (E) Anti-mGluR1β is specific for mGluR1β and does not bind the mGluR1α (Masu et al., 1991) isoform. Representative immunoblots of lysates from HEK293 cells transfected with mGluR1α or mGlu1β and probed with anti-mGluR1β or pan-mGluR1 (Alomone Labs Cat# AGC-006, RRID: AB_2039984) which binds an N-terminal epitope shared by mGluR1 isoforms. (F) Anti-mGluR1β antibody specifically binds endogenous mGluR1β expressed in the cerebellum. Anti-mGluR1β antibody detects mGluR1β monomers, dimers and oligomers in cerebellum lysate from adult wild type but not *mGluR1-/-* mice.

Scale bars: 25 µm (A), 500 nm (B), 2.5 µm (C-C''').

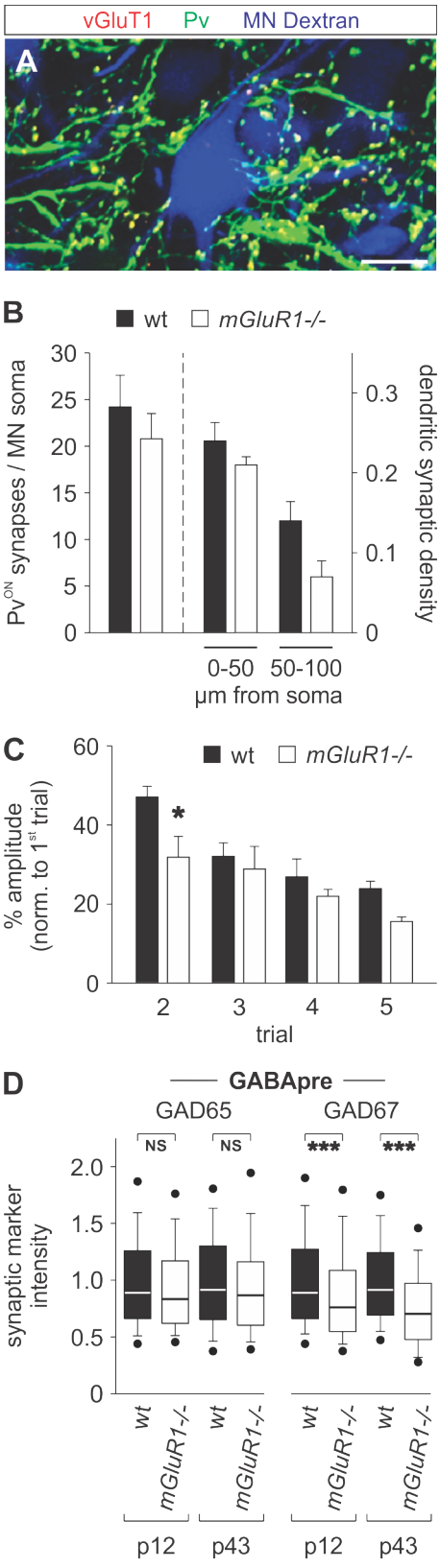

Figure S5. Related to Figure 5: Sensory-motor connectivity and GAD localization in *mGluR1-/-* mice
(A) vGluT1^{ON} (red) and Pv^{ON} (green) sensory afferent terminals contact Cascade Blue dextran backfilled

motor neurons (MN Dextran, blue) in p12 *mGluR1-/-* mice.
(B) The number of Pv^{ON} proprioceptive afferent terminals on the entire motor neuron soma and proximal dendrites (0-50 and 50-100 µm distance from the motor neuron soma) is unchanged in *mGluR1-/-* mice (MN soma: *n*(wt) = 12 soma, 12 mice; *n*(*mGluR1-/-*) = 10 soma, 10 mice; t-test, $p = 0.46$ NS; 0-50 µm dendritic segment: *n*(wt) = 7 soma, 7 mice; *n*(*mGluR1-/-*) = 10 soma, 10 mice; t-test, $p = 0.18$ NS; 50-100 µm dendritic segment: *n*(wt) = 7 soma, 7 mice; *n*(*mGluR1-/-*) = 7 soma, 7 mice; t-test, $p = 0.17$ NS).
(C) Quantification of the monosynaptic reflex amplitude at different trials (stimulation frequency: 1 Hz) as a percentage of the first trial. The reflex is largely unchanged in p12 *mGluR1-/-* as compared to wt mice (*n*(wt) = 3 recordings, 3 mice; *n*(*mGluR1-/-*) = 3 recordings, 3 mice; t-test, $p = 0.039$ * (2nd trial), 0.56 NS (3rd trial), 0.28 NS (4th trial), 0.053 NS (5th trial)).
(D) GAD65 and GAD67 intensity measurements in GABApre terminals of p12 and p43 *mGluR1-/-* mice. While GAD65 levels are not significantly reduced in p12 and p43 *mGluR1-/-* as compared to wt mice, GAD67 levels are similarly reduced at p12 and p43. Data shown normalized with respect to wt data (p12 GAD65: *n*(wt) = 300 boutons, 3 mice; *n*(*mGluR1-/-*) = 300 boutons, 3 mice; Mann-Whitney Rank Sum, $p = 0.0936$ NS; p12 GAD67 *n*(wt) = 300 boutons, 3 mice; *n*(*mGluR1-/-*) = 300 boutons, 3 mice; Mann-Whitney Rank Sum, $p < 0.001$ ***; p43 GAD65: *n*(wt) = 300 boutons, 3 mice; *n*(*mGluR1-/-*) = 400 boutons, 4 mice; Mann-Whitney Rank Sum, $p = 0.0502$ NS; p43 GAD67: *n*(wt) = 300 boutons, 3 mice; *n*(*mGluR1-/-*) = 400 boutons, 4 mice; Mann-Whitney Rank Sum, $p < 0.001$ ***).
Scale bar: 10 µm (A). Error bars represent s.e.m. Lines and whiskers on box diagrams represent data between 9th and 91st percentile, dots show the 5th and 95th percentile.

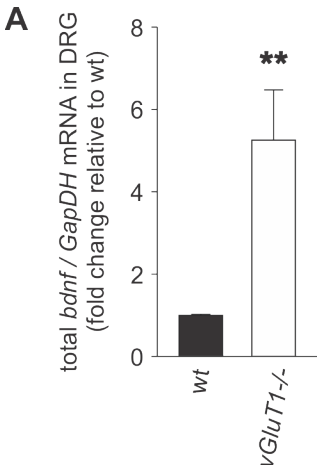

Figure S6. Related to Figure 7: Viral BDNF overexpression
(A) Total *bdnf* mRNA levels in DRG of *vGluT1-/-* mice injected with AAV2/9-GFP-BDNF are ~5-fold higher compared to wt mice (n(wt) = 33 DRG, 5 mice; n(*vGluT1-/-* +BDNF) = 35 DRG, 5 mice; t-test, p = 0.008 **).
Error bars represent s.e.m.

SUPPLEMENTAL EXPERIMENTAL PROCEDURES. REFERS TO EXPERIMENTAL PROCEDURES.

Mouse Strains

To detect disruption of the mGluR1 gene, we used LacZ primers as described in Heinbockel et al., 2004 (Heinbockel et al., 2004). To distinguish between homozygous and heterozygous *mGluR1* mutant mice, we designed an additional primer pair, which annealed in the 7th and 8th intron flanking the exon in which LacZ was introduced. The oligonucleotides are 5' TTTAGAATTACATTTCACCAGTGC (Grm1_genomic_fw1) and 5' CATGATTCTTGCTGTTTCAAAGG (Grm1_genomic_rev4) and generate a 1447-bp wt band. The mutant band is too large to be amplified.

Immunohistochemistry

The following primary antibodies were used at indicated working dilutions: goat anti-ChAT 1:200 (Millipore Cat# AB144, RRID: AB_90650), goat anti-CTb 1:1000 (List Biological Laboratories Inc. Cat# 703, RRID: AB_10013220), rabbit anti-GAD65 1:8000 (Betley et al., 2009), mouse anti-GAD67 1:10000 (Millipore Cat# MAB5406, RRID: AB_2278725), chicken anti-GFP 1:1000 (Millipore Cat# AB16901, RRID: AB_90890), chicken anti-GFP (Aves Labs Cat# GFP-1020, RRID: AB_10000240), rabbit anti-mGluR1β C8 1:1000 (raised against the peptide CPSAHAQL, a partial sequence of mGluR1β C20, RRID: AB_2571735), rabbit anti-mGluR1β C20 1:1000 (raised against the peptide KKRQPEFSPSSQCPSAHAQL corresponding to the distal-most portion of the carboxyl-terminal tail of rat mGluR1β, RRID: AB_2571736; (Francesconi et al., 2009; Kalinowska et al., 2015)), goat anti-Pv 1:2000 (Swant Cat# PVG 214, RRID: AB_10000345), mouse anti-Syt1 1:100 (DSHB Cat# mAb 48 (asv 48), RRID: AB_2199314), rabbit anti-Shank1a 1:64000 (Betley et al., 2009), goat anti-vAChT 1:2000 (Millipore Cat# AG260, RRID: AB_10000324), guinea pig anti-vGluT1 1:32000 (Betley et al., 2009), rabbit anti-vGluT1 1:16000 (Betley et al., 2009), guinea pig anti-vGluT2 1:3000 (Millipore Cat# AB5907, RRID: AB_2301731), rabbit anti-vGluT3 1:1000 (Synaptic Systems Cat# 135203, RRID: AB_10015218), guinea pig anti-vGluT3 1:1000 (Seal et al., 2009).

Histochemistry

Gad65 and *Gad67* probes were previously published (Betley et al., 2009). *mGluR1-8* probes were generated by polymerase chain reaction (PCR) from p5-p11 mouse spinal cords with the antisense probe length ranging from 407 to 825 base pairs and compared with published expression pattern in Allen Brain Atlas.

Synaptic measurements

Density measurements

Only whole cell bodies acquired in several optical planes in the z-axis were included. To calculate the density of proprioceptive terminals on motor neuron dendrites, the numbers of Pv^{ON} contacts within two dendritic compartments (0-50 and 50-100 μm from the soma) were divided by the total length of the dendritic compartment. For GABApre terminals, combinatorial expression of GAD65, GAD67 or Syt1 was analyzed on Pv^{ON} or CTb^{ON} proprioceptive terminals.

Staining intensity measurements

The number of terminals was analyzed within a 10 μm confocal z-stack (300 nm step size). Only terminals localized entirely within the confocal z-stack were included in the analysis. Surface area and staining intensities were determined using Leica LAS AF imaging software. Relative synaptic protein levels were quantified by assessing the mean gray values, defined as the sum of the gray values of all the pixels in a region of interest (pixel sum), divided by the number of pixels in that region (pixel count). Regions of interest were defined as the outline of positively stained varicosities. vGluT1 measurements in *vGluT1* mutant mice were gaited to CTb^{ON} terminals. For quantifying relative levels of GABApre synaptic proteins, only varicosities directly juxtaposed to proprioceptive afferent terminals were considered. Proprioceptive afferent terminals in *vGluT1* mutant mice were identified as either CTb^{ON} terminals or Pv^{ON}/GFP^{ON} terminals. GAD levels were quantified on Pv^{ON}/GFP^{HIGH} terminals.

EM immunohistochemistry and analysis

The following dilutions of antisera were used: goat anti-CTb 1:5000 (List Biological Laboratories Inc.), chicken anti-GFP 1:1000 (Millipore), rabbit anti-mGluR1β C20 1:400 (Francesconi et al., 2009). Processes containing CTb or GFP were immunoperoxidase-(ImP)-labeled with the avidin-biotin-peroxidase complex method. Biotinylated secondary antibodies (Jackson Labs) were used at 1:400 dilution. *Gad65-^{N45}GFP* sections were further processed for immunogold-(ImG)-labeling using 1 nm gold-particle conjugated goat anti-rabbit IgG (Electron Microscopy Sciences Inc.) at 1:50 dilution. ImG labeling was intensified using the silver intensification IntenSE-M Kit (Amersham).

Random immunolabeled sections through the motor neuron nucleus in the ventral-lateral spinal cord were selected, osmicated, dehydrated, and embedded in Embed 812 (Electron Microscopy Sciences Inc.). Ultra-thin sections (65 nm) were collected, counterstained, and examined on a Tecnai electron microscope (FEI Company). Sections passing through the plastic/tissue interface were examined, and digital images of all CTb^{ON} pre- and postsynaptic processes forming synapses in random fields within select grid squares adjacent to the interface were captured at magnifications from 10000x to 49000x. Gray-scale images were processed using Adobe Photoshop CS3 (Adobe Systems Inc.). For dual immunolabeling, images of all GFP^{ON} axonal and terminal processes in randomly selected fields were captured and characterized in terms of the number and subcellular location of mGluR1β-ImG particles. Appropriate controls with omission of primary antibodies were also conducted, but not reported.

Pre-embedding EM dual immunolabeling of mGluR1β was selected because – while less sensitive than other approaches – the position of immunogold particles resulting from this technique reliably reflects the subcellular location of the antigen studied (Pierce et al., 2009). Pre-embedding labeling yields extremely low levels of non-specific, background immunogold labeling: with omission of the primary antibody, and using the same secondary antibody dilutions employed in this study, non-specific labeling has been estimated to represent only 3% of all gold particle labeling (Wang et al., 2003).

Additionally, comparable sections from *Gad65-^{N45}GFP* control mice and *Gad65-^{N45}GFP*; *vGluT1-/-* mice (p21) were processed as described, for single EM ImP-labeling, to visualize GFP. For each experimental condition, > 22 terminals from 3 mice were analyzed. All vesicles in the terminal profile were counted and normalized to terminal area (vesicles/μm^2). Select *Gad65-^{N45}GFP* tissue sections were also processed to ImG-label mGluR1β, and regions containing GABApre interneuron somata were examined, as described.

Electrophysiology

P12 mice were anaesthetized by hypothermia, decapitated and quickly eviscerated. The spinal cord was dissected free and hemisected for better oxygenation under cold (16 ^{o}C) artificial cerebrospinal fluid (aCSF) containing in mM: 128.35 NaCl, 4 KCl, 0.58 $NaH_2PO_4.H_20$, 21 $NaHCO_3$, 30 D-Glucose, 1.5 $CaCl_2.H_20$, and 1 $MgSO_4.7H_20$. The spinal cord was then transferred to a customized recording chamber. The preparation was perfused continuously with oxygenated (95% O_2 and 5% CO_2) aCSF (~13 ml/min) at room temperature. Dorsal roots were stimulated at 1.2, 1.5, 2, 5 and 10x threshold. The stimulus threshold was defined as the current at which the minimal evoked response was recorded in 3 out of 5 trials. Ventral root recordings were fed to an A/D interface (Digidata 1320A, Molecular Devices) and acquired with Clampex (v10, Molecular Devices). Data were analyzed off-line using Clampfit (Molecular Devices). Analysis was performed by averaging 3 to 10 traces. Measurements were made on averaged traces (3-10 trials). Extracellular recordings (Cyberamp, Molecular Devices; amplified 1000x and acquired at DC - 1 or 3 KHz) were obtained from L5 ventral roots in response to stimuli (duration 0.2 ms) from the L4 and/or L5 dorsal roots (depending on the conditioning experiments) delivered by one or two stimulus isolators (A365 - WPI, Sarasota, FL). The temperature of the physiological solution was between 24-25 ^{o}C. Bicuculline, strychnine and CPCCOEt were purchased from Tocris. Bicuculline (10 μM) and strychnine (1 μM) were dissolved directly in aCSF, whereas CPPCCOEt was dissolved in DMSO initially at 50 mM stock concentration and subsequently at 50 μM as the working dilution. Recordings were collected 30 min after application of the drugs.

Transfection and Western blot analysis

HEK293 cells were transfected with Lipofectamine 2000 (Invitrogen) according to manufacturer's conditions. After 48 h, cells were lysed in buffer of 50 mM Tris-HCl (pH 7.4), 150 mM NaCl, 1 mM EDTA supplemented with 1% NP-40, 1% sodium deoxycholate, 0.1% SDS and protease inhibitors.

Microdissected cerebella were sonicated in ice-cold lysis buffer and resulting lysate centrifuged at 20,000 x *g* for 15 min. Equal amounts of cell or tissue lysates were separated by SDS-PAGE and transferred to nitrocellulose membrane according to standard procedures. Immunolabeled proteins were detected by enhanced chemiluminescence.

BDNF ELISA

Mature BDNF (mBDNF) protein levels were quantified using the BDNF E_{max} ImmunoAssay System kit (Promega Cat# G7611, RRID: AB_2571723) with recombinant mBDNF as a standard. Protein was extracted and quantitated following the manufacturer's protocol. Briefly, mice were sacrificed and the caudal portion of the lumbar spinal cord was dissected. Tissue was lysed and homogenized using a dounce homogenizer in lysis buffer (150 mM NaCl, 1% Triton X-100, 25 mM HEPES, 2 mM NaF) containing phosphatase and protease inhibitors. Tissue samples and mBDNF protein standards were loaded in duplicate onto a 96 well plate that had been coated with mouse anti-BDNF monoclonal antibody (1:1000) and blocked with block and sample buffer. A second coating of primary anti-human BDNF polyclonal antibody (1:500) was added to the plate followed by anti-IgY horseradish peroxidase conjugate. The colorimetric reaction was initiated by addition of tetramethylbenzidine chromagenic substrate for 10 mins and stopped with 1N hydrochloric acid. The absorbance was measured at 450 nm on a plate reader (iMark Absorbance Microplate Reader, Bio-Rad Laboratories, Hercules, CA, USA). BDNF concentration (pg BDNF protein/mg of total protein) in tissue samples was calculated using values obtained from the BDNF protein standard curve.

Real time RT-PCR

Primers for *bdnf* exon IX were synthesized by Integrated DNA Technologies (Coralville, IA) and included forward: 5'-TCATACTTCGGTTGCATGAAGG-3' and reverse: 5'-AGACCTCTCGAACCTGCCC-3' primers. Primers for GAPDH (QT01658692) were purchased from Qiagen (Valencia, CA).

SUPPLEMENTAL REFERENCES

Francesconi, A., Kumari, R., and Zukin, R.S. (2009). Proteomic analysis reveals novel binding partners of metabotropic glutamate receptor 1. J Neurochem 108, 1515-1525.

Heinbockel, T., Heyward, P., Conquet, F., and Ennis, M. (2004). Regulation of main olfactory bulb mitral cell excitability by metabotropic glutamate receptor mGluR1. Journal of neurophysiology 92, 3085-3096.

Kalinowska, M., Chavez, A.E., Lutzu, S., Castillo, P.E., Bukauskas, F.F., and Francesconi, A. (2015). Actinin-4 Governs Dendritic Spine Dynamics and Promotes Their Remodeling by Metabotropic Glutamate Receptors. The Journal of biological chemistry 290, 15909-15920.

Masu, M., Tanabe, Y., Tsuchida, K., Shigemoto, R., and Nakanishi, S. (1991). Sequence and expression of a metabotropic glutamate receptor. Nature 349, 760-765.

Seal, R.P., Wang, X., Guan, Y., Raja, S.N., Woodbury, C.J., Basbaum, A.I., and Edwards, R.H. (2009). Injury-induced mechanical hypersensitivity requires C-low threshold mechanoreceptors. Nature 462, 651-655.

Tanabe, Y., Masu, M., Ishii, T., Shigemoto, R., and Nakanishi, S. (1992). A family of metabotropic glutamate receptors. Neuron 8, 169-179.

Wang, H., Cuzon, V.C., and Pickel, V.M. (2003). Postnatal development of mu-opioid receptors in the rat caudate-putamen nucleus parallels asymmetric synapse formation. Neuroscience 118, 695-708.